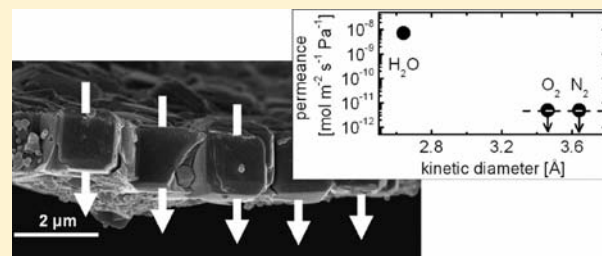


# Bicontinuous Zeolite Polymer Composite Membranes Prepared via Float Casting

Ina Kiesow, Dawid Marczewski, Lutz Reinhardt, Marcel Mühlmann, Mario Possiwan, and Werner A. Goedel\*

Physical Chemistry, Chemnitz University of Technology, Strasse der Nationen 62, 09111 Chemnitz, Germany

**ABSTRACT:** We prepared bicontinuous composite membranes comprising zeolite A particles. The particles form a monolayer which is embedded in a polymer sheet in such a way that each particle penetrates both surfaces of the polymer sheet. Preparation was done via “float casting”; a mixture of hydrophobized zeolite particles and an appropriate volume of a nonvolatile polymerizable organic liquid monomer was applied onto a water surface. The monomer was solidified via photopolymerization to form the above-mentioned membrane. In as-prepared state (without extensive drying), this membrane is permeable for water vapor (in case of zeolite 4A permeance =  $8 \times 10^{-9} \text{ mol m}^{-2} \text{ s}^{-1} \text{ Pa}^{-1}$ , permeability =  $1.65 \times 10^{-14} \text{ mol m}^{-1} \text{ s}^{-1} \text{ Pa}^{-1} = 49 \text{ barrer}$ ) but impermeable for nitrogen (permeance below detection limit of  $5 \times 10^{-12} \text{ mol m}^{-2} \text{ s}^{-1} \text{ Pa}^{-1}$ , permeability below detection limit of  $1 \times 10^{-17} \text{ mol m}^{-1} \text{ s}^{-1} \text{ Pa}^{-1} = 0.03 \text{ barrer}$ ). The permeance for water vapor increases with increasing pore size of the zeolite (in case of zeolite 5A, all other parameters being unchanged, permeance =  $12 \times 10^{-9} \text{ mol m}^{-2} \text{ s}^{-1} \text{ Pa}^{-1}$ , permeability =  $2.4 \times 10^{-14} \text{ mol m}^{-1} \text{ s}^{-1} \text{ Pa}^{-1} = 72 \text{ barrer}$ ). These observations indicate that the water molecules are predominantly transported through the zeolite channels and at the same time block the passage of other molecules. The impermeability for nitrogen in as-prepared state indicates a low amount of defects that are not blocked by water. Furthermore, the composite nature of the membrane gives rise to a reduced brittleness; membranes can be handled manually without support structure and thus might be promising candidates for separation technology.



## 1. INTRODUCTION

Separation of mixtures and purification of raw products are essential operations in natural and industrial processes. Compared to other processes, like distillation, membrane separation technology is more economical, because no heating or cooling is needed, and more efficient, as it is even able to split up azeotropic mixtures. A wide field of materials is used to prepare separation membranes, porous or non porous, organic as well as inorganic. The search for highly selective materials and their efficient implementation in membranes is continuously in progress and is a big challenge for science.

The selectivity of a membrane is usually based either on a selective absorption or on a difference in the mobility of the permeating substances. Especially in rigid materials with Ångström size pores, the mobility strongly depends on the size of the permeating molecules. Hence, molecular sieves like zeolites particularly attract the researchers' attention. Zeolites are comparatively cheap crystalline materials characterized by a regular system of inner channels and uniform open pores. Their sharp pore size distribution provides the best conditions for a high selectivity. Furthermore, some zeolites preferentially absorb small molecules within their channels based on polarity or short-range interactions and thus offer selective transport based on selective adsorption.

Therefore, much effort is invested to generate zeolite membranes.<sup>1,2</sup> Zeolite membranes are not only used for size-

selective separations, like the splitting up of isomeric mixtures,<sup>3</sup> but also for separations based on polarity, like the dehydration of organic liquids<sup>4,5</sup> and gases.<sup>5</sup> Conventionally they are prepared by hydrothermal processes/seeded growth, are purely inorganic and polycrystalline, and have limited mechanical stability.<sup>1,6,7</sup> Thus, zeolite membranes usually are not used as self-supporting membranes but are grown on top of a rigid macroporous support and never separated from it. They may contain defects, e.g., nonzeolitic pores or mesopores,<sup>8,9</sup> usually arising along grain boundaries. One may close these defects by infiltration after membrane preparation, e.g., by wet impregnation with an initiator followed by vapor-phase deposition of a polymer.<sup>10</sup>

Flexible self-supporting membranes can be prepared by embedding selective particles within a nonselective (or less-selective), tough matrix to create so-called “mixed matrix membranes.”<sup>11,12,7,13–16</sup> To prepare such membranes, often particles of selective materials are mixed with a solution of an organic polymer, and these mixtures are cast onto a support, dried, and separated from the substrate to yield a mechanically stable self-supporting membrane. The thickness of these so-called mixed matrix membranes usually is significantly larger than the diameters of the embedded particles, and most

Received: December 3, 2012

Published: February 12, 2013

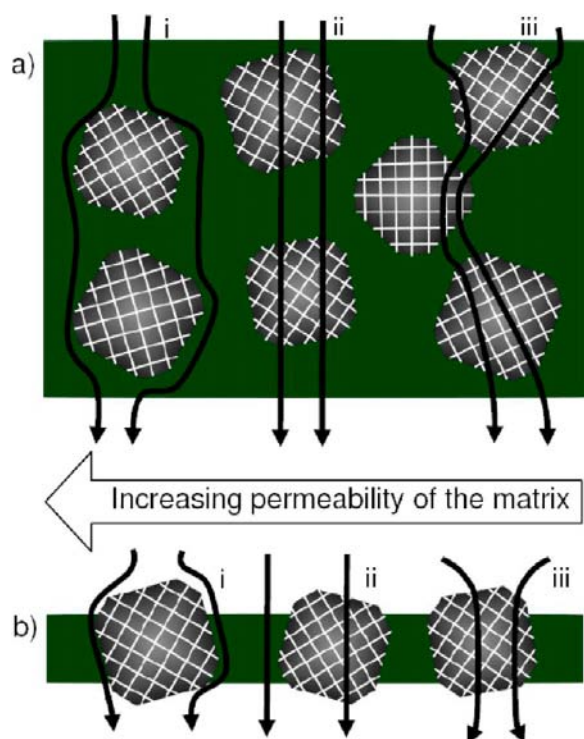


**Figure 1.** Comparison of (a) three-dimensional and (b) lateral embedding of a selective component within a nonselective matrix of a membrane (permeability of the matrix increasing from right to left); only in case (b,iii) the matrix has no influence on the selectivity of the membrane.

particles are completely surrounded by the polymer matrix (see Figure 1a). Thus, the selectivity is strongly influenced by the matrix.<sup>7</sup> A nonselective matrix of a high permeability provides preferred pathways through the membrane by which permeating substances can circumvent the embedded selective material (Figure 1a,i), whereas a nonselective matrix of a low permeability not only retards the flow but also becomes the rate-determining barrier within the membrane (Figure 1a,iii). In both cases the selectivity is dominated by the nonselective matrix. Even if the permeability of the matrix is optimized to match that of the particles, the theoretically calculated as well as experimentally observed selectivity of the membrane is less than the selectivity of the pure embedded phase.<sup>7,14,17</sup> Furthermore, one often observes that interactions between the particles and the matrix give rise to a layer of rigidified polymer or reduced permeability.<sup>14</sup>

Thus, we suggest here an alternative principle: A membrane that is composed of particles that are embedded within a tough polymer matrix only at their sides and not at the top and bottom (see Figure 1b). In such a bicontinuous geometry, one may choose an impermeable matrix, thus diminishing flow that circumvents the particles, however, without creating rate-determining barriers composed of the matrix (Figure 1b,iii). Thus, one might obtain a mechanically stable freestanding membrane that has the selectivity of the embedded particles, but has no defects due to grain boundaries.

There are concepts to reduce the thickness of zeolite/polymer mixed matrix membranes by inclusion of the zeolite particles within a polymer layer created by interfacial polymerization. In this technique, the membrane thickness currently still is larger than the particle diameter.<sup>18,19</sup> An

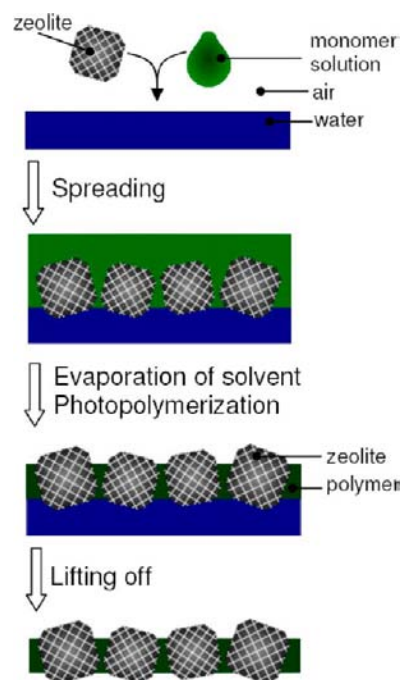


**Figure 2.** Preparation of a bicontinuous zeolite composite membrane with laterally embedded zeolite particles.

alternative technique to prepare a composite membrane as thin as the particle diameters, is float casting. It is schematically illustrated in Figure 2: A mixture of hydrophobized particles, a volatile solvent, and a nonvolatile polymerizable organic liquid monomer is spread onto a water surface. The particles form a monolayer, while the monomer fills the space between the particles due to capillary forces.<sup>20</sup> After the evaporation of the solvent, a thin film of the monomer embeds the particles. If the volume ratio of monomer/particle is chosen correctly, it embeds them in such a way that each particle is embedded laterally but protrudes at the upper and lower interface of this film. Solidification of the monomer by photopolymerization finally yields the desired composite membrane. Until now, the focus of these investigations was the preparation of microsieves; the embedded particles were “dumb”, impermeable silica particles, used as sacrificial porogenes. These porogenes were etched away immediately after solidification to generate a thin polymeric microsieve bearing uniform pores. The internal surface of these pores reflects the shape of the external surface of these submicroscopic particles.<sup>21–23</sup> If the float-casting principle works well with “dumb” sacrificial particles, then one should try it as well using “smart” particles of selective permeability (and leave them in place) to create the desired structure as depicted in Figure 1b. It is the purpose of this contribution to show that this actually can be done.

In order to prepare bicontinuous composite membranes via float casting, we have to choose particles which are readily available in size distributions of acceptable width and offer some selectivity in transport properties between two suitable substances. To test the assumption that transport actually occurs through the particles, one should be able to tune the permeability without affecting any other of the relevant parameters. To ease the transfer of our existing knowledge, we preferred particles that may be hydrophobized in a similar way as we did previously using the “dumb” silica particles. Furthermore, we wanted to be able to compare our results to

data obtained on zeolite membranes that were prepared in the conventional way by seeded growth. We finally settled for particles of zeolite A which to our judgment fulfill these requirements. The way the membrane is prepared via float casting on a water surface, the inner channels of the hydrophilic zeolites A will be filled with water and will block transport of other molecules through the zeolite. Thus, we expect in our composite membrane, selective transport for water vapor compared to other gases, e.g., oxygen or nitrogen.

## 2. EXPERIMENTAL SECTION

**2.1. Materials.** The nonvolatile polymerizable organic liquid monomer HEMATMDI (95% purity) (a mixture of 7,7,9- and 7,9,9-trimethyl-4,13-dioxo-3,14-dioxo-5,12-diaza-hexadecan-1,16-diol-dimethacrylate) was obtained as a gift from Röhm Evonik GmbH, at that time bearing the trade name PLEX 6661-0. It is by now available from Evonik Industries bearing the trade name VISIOMER HEMATMDI. 3-methacryloxypropyltrimethoxysilane (TPM, 97% purity), *n*-octadecyltriethoxysilane (ODES, 98% purity), and 1H,1H,2H,2H-perfluorooctyltriethoxysilane (PFOS, 97% purity) coating agents and benzoinisobutylether as photoinitiator were purchased from Aldrich. All chemicals and solvents were used as received, if not mentioned otherwise. Toluene (technical grade) was dried by storing over zeolite 3A, the latter activated beforehand by heating to 350 °C in air at normal pressure. Zeolites 4A and 5A of identical particle size were kindly provided as a white powder by SILKEM d.o.o., Kidričevo, Slovenija.

The contact angles between the monomer and glass substrates treated with PFOS [ $\Theta(\text{air/monomer/substrate}) \approx 29^\circ \pm 3^\circ$ ;  $\Theta(\text{water/monomer/substrate}) \approx 52^\circ \pm 6^\circ$ ] were determined using a Krüss G2 camera/image analysis system, 30 min after deposition of a droplet of the monomer in either air or in water onto the solid substrate. The high viscosity of the monomer hindered the exact discrimination between advancing and receding contact angles. The values given above are averages obtained from at least four measurements, and errors given are standard deviations.

**2.2. Membrane Preparation.** The zeolite particles were washed with demineralized water and dried in air at 350 °C overnight. Subsequently, they were hydrophobized by immersion overnight in a 10 mM solution of TPM, ODES, or PFOS in toluene, washed with toluene and acetone, and dried at 120 °C. The hydrophobized zeolite particles thus obtained were well dispersed with the aid of ultrasonication in a mixture of ethanol and chloroform (1:1 by mass) in which the appropriate amount of the nonvolatile polymerizable organic liquid monomer HEMATMDI and the photoinitiator (6% by mass with respect to the monomer) was dissolved. In the final mixture the mass fraction of the monomer was varied systematically between 0.002 and 0.25. The mass fraction of zeolite was kept constant at 0.01. An amount of this dispersion appropriate for the formation of a monolayer of zeolites was spread onto a water surface of water filled glass Petri dishes of diameters varying between 4 cm and 13 cm. After spreading, the solvent was allowed to evaporate for approximately 1 h. The water surface that was covered with a layer of particles and monomer was irradiated by a UV low-pressure mercury lamp (Umex, Dresden, principal wavelength 254 nm, intensity 0.08 W/cm<sup>2</sup>). The volume fraction of the polymer in the final membrane was estimated from the mass of the monomer  $m_M$ , the mass of the zeolite  $m_Z$ , and their densities  $\rho_Z$  and  $\rho_M$  as follows: volume fraction =  $(m_M/\rho_M)/(m_M/\rho_M + m_Z/\rho_Z)$ . The corresponding densities were estimated as:  $\rho_M = 1.09 \text{ g cm}^{-3}$  and  $\rho_Z = 1.9 \text{ g cm}^{-3}$ . However we have to point out that the actual densities might deviate from the estimated values. The zeolites comprise a certain amount of water, and the density of the organic phase increases upon polymerization. Furthermore part of the monomer might dissolve in the aqueous subphase. 10  $\mu\text{m}$  thick membranes made out of pure photopolymerized monomer were prepared by dissolving the monomer in ethanol, applying an amount of this solution appropriate to achieve a layer of the desired thickness onto an alumina foil, waiting for 30 min

to let the solvent evaporate, illuminating the monomer layer with ultraviolet light, and dissolving the alumina foil in hydrochloric acid.

**2.3. Characterization.** Scanning electron microscopy (SEM) pictures were taken by using a NanoNovaSEM (Philips). Non-conductive samples were coated by high-vacuum sputtering with a layer of palladium, respectively, gold of 10 nm to 20 nm thickness. To obtain lateral pressure to area isotherms of zeolite A particles, a dispersion of the particles in an ethanol–chloroform mixture (mass fraction of particles = 0.04, mass fraction of chloroform = 0.48, mass fraction of ethanol = 0.48) was applied to the surface of a water filled Langmuir-trough equipped with a floating barrier for the detection of the lateral pressure (LAUDA FW2).

Water adsorption–desorption measurements of the coated particles exceeding temperatures of 100 °C (Figure 4 c,d) were performed by means of a thermogravimetric analyzer TGA7 (Perkin-Elmer). Before and during each experiment the microbalance was purged with nitrogen humidified at room temperature with a constant degree of relative humidity of 33% by bubbling through a saturated MgCl<sub>2</sub> solution. Before starting the temperature program, the chamber was purged at room temperature until a constant mass of the zeolite sample was obtained. Thermogravimetry of zeolites and membranes at temperatures below 100 °C (Figure 9b) were performed with the same thermogravimetric analyzer. The nitrogen was saturated with water by bubbling through water kept at the same temperature as the sample.

Permeabilities of the membranes were determined by single gas permeation in case of oxygen and nitrogen and vapor permeation in case of water: A homemade permeation unit was used into which a stainless steel permeation cell (kindly provided by mecadi GmbH, Bexbach, Germany) was integrated. The permeation cell comprised two chambers: the feed chamber and the permeate chamber. Each of these two chambers was equipped with a pressure transducer (GEMS Sensors), and the volumes of both chambers were determined from the pressure change occurring upon filling them with a known amount of nitrogen, assuming ideal gas behavior. The membrane was sandwiched between two sheets of adhesive alumina foil tape which had a circular hole in their center. The space between membrane and aluminum foil was sealed by a two-component epoxy resin adhesive (UHU-Plus schnellfest). The sandwich was mounted within the permeation cell in such a manner that it separated the feed chamber from the permeate chamber. It was supported on the permeation side by a porous metal plate and sealed at the perimeter by a Viton ring. The permeation study was realized by using nitrogen gas, oxygen gas (both gases of 99.99%+ purity) and water vapor provided by a thermostatted water reservoir. The whole system including feed and permeate side was evacuated overnight before each measurement. In case of nitrogen and oxygen permeation, the feed side was loaded with gas using pressures varying from 20 mbar to 1 bar regulated by a pressure controller. In case of water vapor permeation, the feed side was loaded with water vapor emanating from a supply vessel filled with degassed water and connected to the feed side of the permeation unit via Teflon tubing. To ensure uniform filling by the water vapor, water vapor was pumped from the supply vessel through the feed chamber of the permeation unit. A valve between feed chamber and pump was used to regulate the pressure of the water vapor inside the feed chamber. During measurement the valve was almost closed, and as a result the pressure in the feed chamber was the same as can be expected from the partial pressure of water at the used temperature. The permeation cell and the supply vessel were placed into a thermostatted air cabinet kept at a constant temperature (at 23 °C, unless stated otherwise in the following text). After filling the feed chamber, the valve between the permeate side and the pump was closed, and the pressure was monitored. The permeance was calculated from the pressure rise occurring in the permeate chamber, taking into account the volume of the permeate chamber and assuming ideal gas behavior of the permeate.

## 3. RESULTS AND DISCUSSION

The pristine zeolite particles to be used for membrane preparation are shown in Figure 3a. From image analysis of



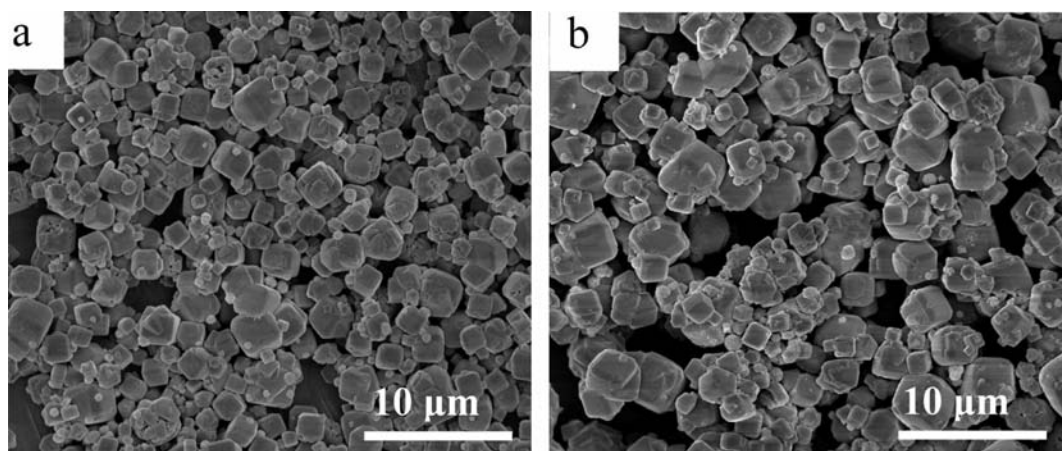


Figure 3. Scanning electron microscopy (SEM) images of the zeolite particles (a) before and (b) after coating with PFOS.

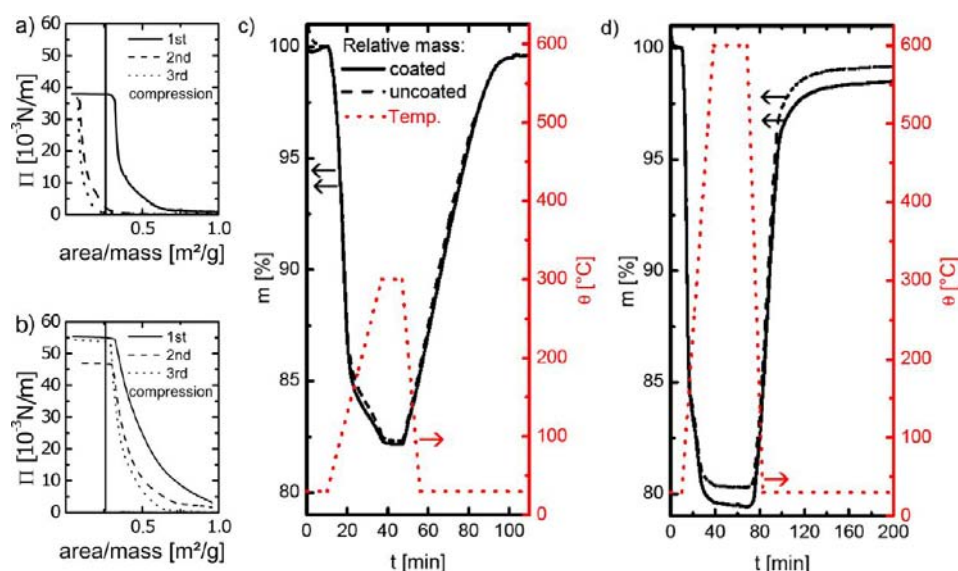
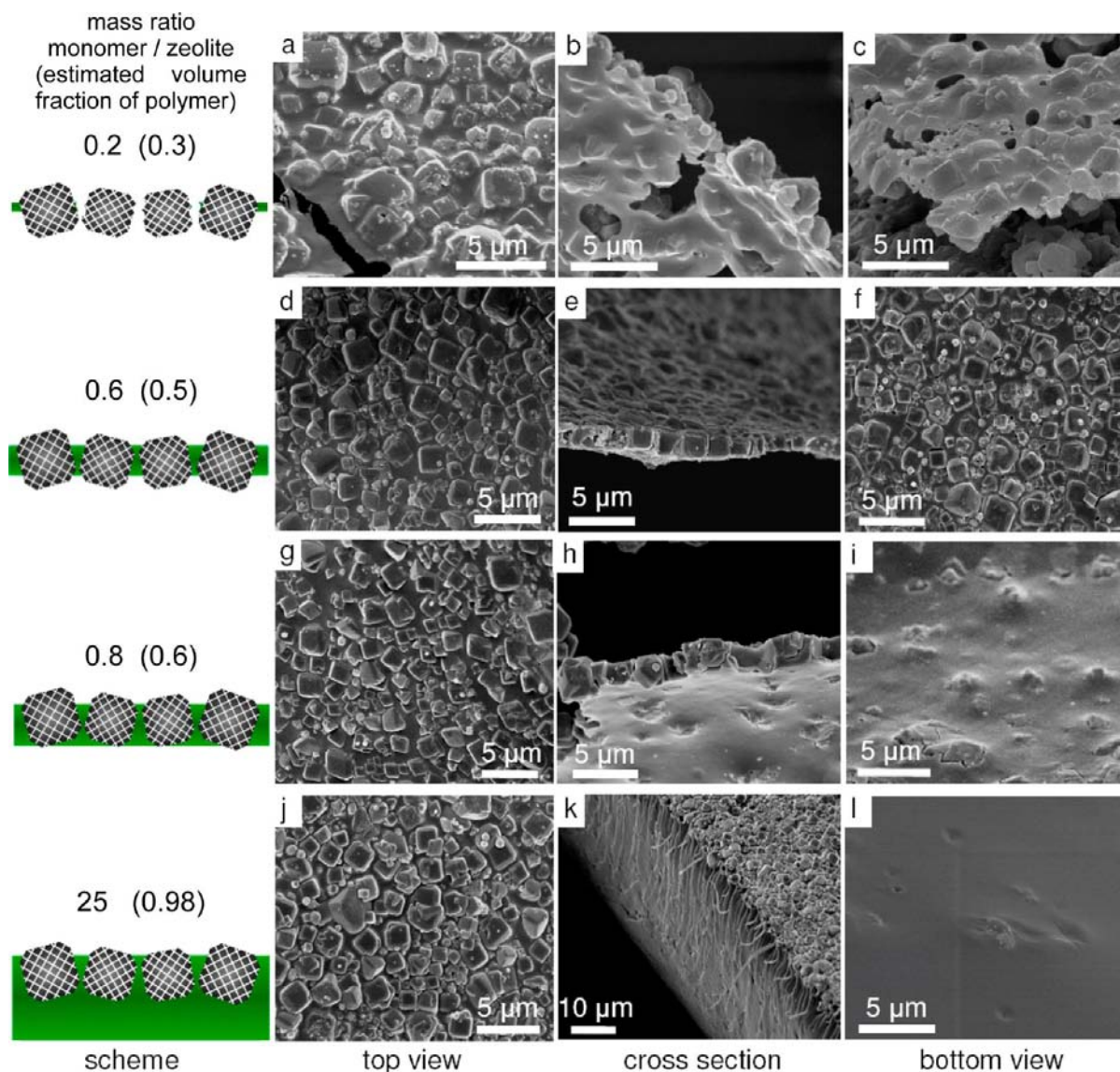


Figure 4. (a,b) Isotherms of lateral pressure to specific area of zeolite particles on water coated with the (a) acrylic silane TPM and (b) perfluorooctyl silane PFOS. Three compressions were recorded in one series (first compression, solid line; second compression, dashed line; third compression, dotted line). The theoretical specific area of densely packed particles is illustrated by a vertical line at approximately  $0.25 \text{ m}^2/\text{g}$ . (c,d): Thermogravimetry of zeolites uncoated (dashed line) and coated with the perfluorooctyl silane PFOS (solid line) heated up to (c)  $300 \text{ }^\circ\text{C}$  and (d)  $600 \text{ }^\circ\text{C}$  and subsequently cooled in moist air. The fully reversible mass loss in (c) is an effect of desorption–adsorption processes of water out of/ into the zeolite channel system.

such electron microscopy images we calculate an average width of a particle of  $(1.8 \pm 0.4) \mu\text{m}$ , an average area per particle of  $(3.5 \pm 1.6) \mu\text{m}^2$ , and an average particle volume of  $(7.2 \pm 4.9) \mu\text{m}^3$ .<sup>24</sup> The successful preparation of the desired zeolite composite membranes via float-casting critically depends on suitable contact angles between the monomer, water, and particles (see Figure 2).<sup>20</sup> Hydrophilic particles are not suitable. Therefore, in the first step, the zeolite particles had to be coated by a silane coupling agent. We expected the zeolite particles to react with silane coupling agents the same way as silica particles. Thus, three silane compounds already successfully applied to silica particles in previous papers<sup>20</sup> were used for this coating (in the order of increasing hydrophobicity): 3-methacryloxypropyltrimethoxysilane (TPM), n-octadecyltriethoxysilane (ODES) and 1H,1H,2H,2H-perfluorooctyltriethoxysilane (PFOS). As an example, Figure 3b displays zeolite particles before and after the coating is essentially the same. (As a side

effect, submicrometric dust particles are washed out.) However, in contrast to pristine particles, the coated particles do not submerge if applied to a water surface.

To discriminate the degree of hydrophobization obtained by the coating and to select the most suitable coating, the particles were applied to a Langmuir trough (see Figure 4a,b). The particles were dispersed in a mixture of chloroform and ethanol, were spread evenly onto a water-filled Langmuir trough, and the corresponding lateral pressure to area isotherms were recorded. The pristine particles gave rise to irreproducible isotherms without a clear collapse and a lateral pressure not exceeding  $20 \times 10^{-3} \text{ N/m}$  (data not shown). ODES and TPM coatings led to almost identical isotherms (see Figure 4a for the case of TPM). The first compression yielded a smooth rise of the lateral pressure and a collapse close to the specific area of a monolayer calculated theoretically. However, the second and third isotherm showed a collapse at a significantly lower area. Thus, at the collapse a part of the particles is irreversibly



**Figure 5.** SEM images of zeolite composite membranes prepared via float casting on a water surface, as shown schematically in Figure 2. From top to bottom row using increasing volume fractions of the monomer (= increasing polymer layer thickness): first column is schemes of the particle position within the layer, and second through fourth columns are top, cross section, and bottom views of the corresponding membranes.

removed from the water surface. In the case of particles coated with PFOS—the silane bearing perfluoroalkyl side chains—one observes a very similar isotherm in the first compression and an almost complete recovery of the monolayer even in the second and third compression (Figure 4b). Obviously PFOS-coated particles give rise to the most stable monolayers. Thus, they were selected for the following experiments.

Although the silane coating is needed to adjust the contact angles, it might adversely affect or block the channels of the zeolites. Given the hydrophilic nature of the selected type of zeolite, we expected that the channels were filled with water. In view of this, the silanes did not have access to the interior of the channels. However, the entrance might be blocked by the coating.

Thus, to convince ourselves that the channels are still open after the coating, water adsorption–desorption experiments were performed (see Figure 4c,d). The zeolite particles were placed in a thermogravimetric analyzer (TGA) that was purged with nitrogen of 33% relative humidity and subjected to

heating–cooling cycles which shift the temperature-dependent adsorption equilibrium between zeolites and the surrounding atmosphere. For example, Figure 4c shows the mass change of uncoated zeolites and zeolites coated with the fluorinated silane PFOS, heated to 300 °C and cooled down again to room temperature in moist atmosphere. Both samples show an almost identical weight loss, completely recover their original weight after cooling and show very similar desorption and absorption kinetics. Thus, we suppose that both samples were saturated with water at the beginning and both lost, and reabsorbed the same amount of water. Therefore, we conclude that the coating does neither clog the pore openings nor hydrophobize the channels and that the water is free to move within the channel system. If heated to 600 °C (see Figure 4d) the weight loss is, as expected, more severe but still similar in both samples.

Given the fact that the particles form stable monolayers and that their capability to absorb water was not affected, we are now in a position to prepare membranes using the procedure



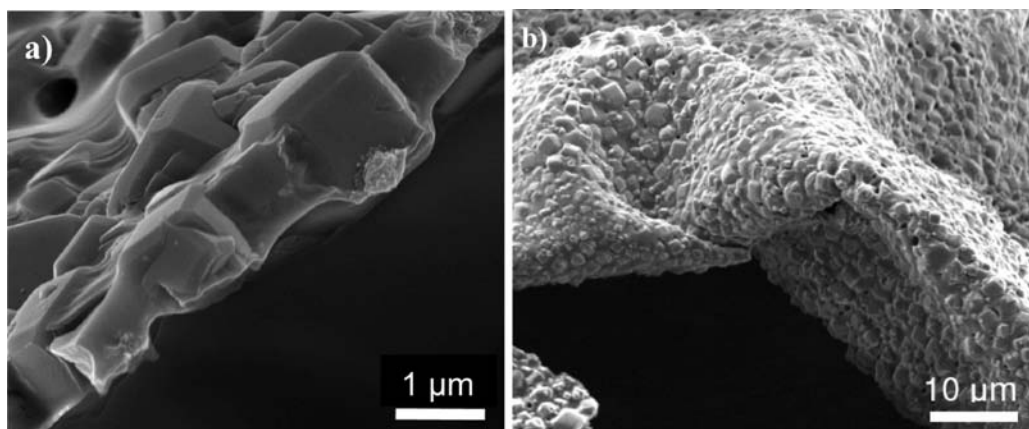


**Figure 6.** SEM images of bicontinuous zeolite composite membranes: (a) close up image of the side of a fractured membrane revealing the finite contact angles and (b) a membrane that was folded to illustrate its flexibility.

shown in Figure 2. A mixture of the coated particles, the monomer and a volatile solvent was spread onto a water surface. After evaporation of the solvent and photopolymerization of the monomer, a composite membrane of uniform thickness was obtained (see Figure 5). This membrane is composed of densely packed zeolite particles that protrude out of the upper surface of the polymer layer. It is possible to control the polymer layer thickness by varying the volume fraction of the monomer in the initial dispersion. When the amount of the monomer is below a characteristic minimum, the obtained membrane is slight and discontinuous and comprises holes of micrometer size (Figure 5a–c). On the other hand, if a very high volume fraction of monomer is used, the thickness becomes larger than the particle size, and the particles are attached to the top side only and do not reach the bottom side of the membrane (Figure 5j–l). If approximately equal volumes of monomer and particles are used, then one obtains a continuous layer and particles touching both interfaces. Slight variations in the amount of the monomer give rise to particles either still covered on one side (Figure 5g–i) or penetrating through both interfaces as desired (Figure 5d–f). Ideally, a high selectivity is desired, thus a transport exclusively through the channel system of the particles is needed. An optimum volume ratio of zeolites and monomer shall give rise to pathways through the zeolite particles but at the same time completely fill the space between the particles and thus block the transport circumventing the particles. Therefore, structures such as shown in Figure 5d–f were the desired ones.

The contact angle of the monomer on planar glass substrates treated with the same coupling agent is finite in air as well as in water. This observation is in agreement with close up SEM images of the sides of fractured membranes, which as well show finite contact angles between the polymer and the particles (Figure 6a). Thus, it is reasonable to assume that the matrix does neither coat the top nor the bottom of the particles but embeds them from the sides only. The membranes show some degree of flexibility. For example Figure 6b shows a piece of a membrane that was folded without breaking. On the other hand, however, the membranes have a tendency to rupture if subjected to lateral stress.

The last point to prove is that the membranes show selective permeability through the zeolites but no significant transport circumventing them. Thus, membranes made out of the pure matrix and membranes with properties, as shown in Figure 5d–f, were mounted within a permeation cell, and the permeance

was determined for various gases. Prior to the permeation measurement, the whole setup was evacuated but not heated. Thus, it is reasonable to assume that the channels of the zeolites are filled with water and blocked for the passage of other gases like air.

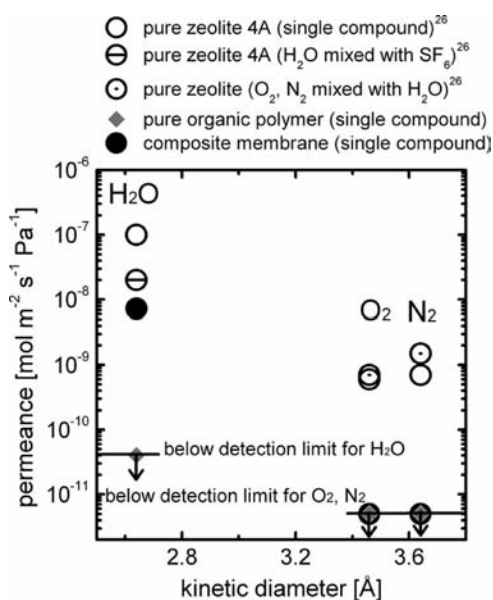


**Figure 7.** Permeances of water, oxygen, and nitrogen through membranes made exclusively out of the polymeric matrix (grey  $\blacklozenge$ ) and composite membranes made from zeolite 4A and polymer such as those shown in Figure 5d–f ( $\bullet$ ) (at 23 °C), compared to the corresponding values of a zeolite 4A membrane of comparable thickness prepared by seeded growth<sup>26</sup> ( $\circ$ ,  $\ominus$ , and  $\odot$ ). (The arrows indicate that the permeance is below the detection limit.)

The corresponding permeances for various gases are displayed and compared to literature data in Figure 7. Membranes made out of the pure matrix had permeances for nitrogen, oxygen ( $<5 \times 10^{-12} \text{ mol m}^{-2} \text{ s}^{-1} \text{ Pa}^{-1}$ ), and water vapor ( $<4 \times 10^{-11} \text{ mol m}^{-2} \text{ s}^{-1} \text{ Pa}^{-1}$ ) below the detection limits (see Figure 7, gray diamonds).<sup>25</sup> Composite membranes comprising zeolite 4A showed again no measurable permeance for nitrogen and oxygen but a clearly measurable permeance for water vapor (permeance =  $8 \times 10^{-9} \text{ mol m}^{-2} \text{ s}^{-1} \text{ Pa}^{-1}$ , permeability = 49 barrer =  $1.65 \times 10^{-14} \text{ mol m}^{-2} \text{ s}^{-1} \text{ Pa}^{-1}$ ). Our

results (filled circles) are in accordance with similar results on zeolite membranes made by conventional seeded growth<sup>26</sup> (indicated in Figure 7 by open symbols). In agreement with the authors of ref 26, we attribute the permeance for water to transport through the continuous channels within the zeolite structure and the impermeability to oxygen and nitrogen to the fact that water absorbed within the channels blocks the passage of other gases. In agreement with this interpretation, adsorption experiments show that water contents of only a fraction of full saturation are sufficient to drastically impede flow of other molecules into zeolite crystals.<sup>27</sup> The permeance of the membranes prepared by conventional seeded growth<sup>26</sup> for water as well as for nitrogen is larger than the permeance of our membrane. In ref 26 parts of the flow were attributed to transport through defects that were too large to be completely filled with water. Such defects provide nonselective pathways through the material and allow other molecules to pass. When these defects were blocked in ref 26 by a 98% excess of a gas of large molecules, such as ethane or sulfur hexafluoride, the permeance of this membrane for water dropped by a factor of 8 to a value of  $20 \times 10^{-9} \text{ mol m}^{-2} \text{ s}^{-1} \text{ Pa}^{-1}$ . Given the fact that the thickness of our membrane is comparable to the thickness of the membrane used in ref 26 and that in our membrane a part of the area is occupied by the impermeable polymer, we consider the permeance of the membrane prepared by seeded growth for water in presence of blocking molecules comparable to the permeance of our composite membrane. However, in our case no blocking with large gas molecules was needed. This interpretation is further supported by the fact that the permeance of our composite membrane for nitrogen is below detection limit and much lower than the permeance of the membrane prepared by seeded growth; again in absence of additional blocking molecules. Thus, it is very likely that our composite membranes have a significantly lower density of defects not blocked by water than zeolite membranes prepared by seeded growth. We attribute this reduced defect density to the fact that the zeolite particles are embedded in a tough but flexible continuous polymer matrix and that the matrix was liquid in an intermediate state of preparation, and thus it was able to snugly surround the particles.

To convince us further that the transport of water occurs predominantly through the particles rather than circumventing them, we varied the pore size and the temperature. The advantage of zeolite A is the fact that one can tune the nominal channel width by simple ion exchange. Thus, in addition to the zeolite 4A with a nominal channel width of 4 Å, we had at our disposition a batch of zeolite 5A with a nominal channel width of 5 Å; all other properties being identical to the previously used batch of zeolite 4A. Thus, if transport occurs predominantly through the channels, it is reasonable to expect membranes prepared with this batch to be more permeable for water than those made from zeolite 4A. This indeed is the case (permeance =  $12 \times 10^{-9} \text{ mol m}^{-2} \text{ s}^{-1} \text{ Pa}^{-1}$ , permeability =  $2.4 \times 10^{-14} \text{ mol m}^{-1} \text{ s}^{-1} \text{ Pa}^{-1} = 72 \text{ barrer}$ ), see as well Figure 8.

Another instructive experiment is the variation of the temperature. Raising the temperature may increase the diffusion coefficient of the permeating substance and thus the permeance of a membrane. However, if permeation involves an exothermic absorption equilibrium, raising the temperature may as well deplete the membrane of the permeating substance to such an extent that permeance is lowered.<sup>28,29</sup> Upon raising the temperature, Aoki, Kusakabe, and Morooka observe increasing as well as decreasing water permeances of zeolite membrane.<sup>26</sup>

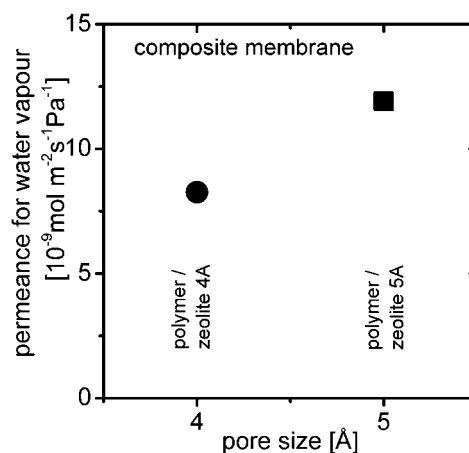


**Figure 8.** Permeances of water (at 23 °C) through membranes made out of the polymeric matrix and zeolite 4A (●), and made out of the polymeric matrix and zeolite 5A (■).

Zhu, Gora, van den Berg, Kapteijn, Jansen, and Moulijn observe increasing permeances,<sup>28</sup> while Sato, Sugimoto, and Nakane report a decreasing permeance.<sup>30</sup> The discrepancy between these observations most likely is due to the fact that the partial pressures and temperatures used were not identical in these investigations. As can be seen from Figure 9a, the permeance of the composite membrane in our case decreases upon raising the temperature, although our conditions are closer to those used in ref 28 than to those used in ref 30. The reason for this discrepancy is not completely understood yet. Nevertheless, the decrease in permeance most likely has to be connected to desorption of water. As can be seen in Figure 9b, raising the temperature of zeolites, the polymer matrix and the corresponding composite membranes in equilibrium with moist atmosphere indeed give rise to a weight loss. The zeolites lose weight more pronounced than the polymer matrix. We take this latter fact and the observed decrease in permeance upon raising the temperature as an additional indication that transport occurs predominantly via the zeolite particles.

#### 4. CONCLUSION

In summary, we can conclude that float casting is an effective way to prepare thin bicontinuous zeolite polymer composite membranes. We successfully optimized the thickness of the embedding polymer layer to such an extent that each of the particles protrudes at the upper and bottom surfaces of the polymer layer and provides pathways directly through the selective zeolite particles. The selectivity of the composite membrane, especially its dependence on the nominal channel width of the zeolites and on temperature, indicates that transport occurs predominantly through the particles and that the matrix does not impose a rate-determining barrier to transport. As the membrane in a non-dried state is impermeable for nitrogen and oxygen but has a permeance for water that is comparable to zeolite membranes prepared by seeded growth, we assume that the amount of defects not blocked by water is comparatively low.

The scope of this paper was to show that the new principle of membrane preparation, float casting of mixtures of particles and polymerizable liquids, works and gives rise to thin bicontinuous composite membranes. In such membranes transport occurs predominantly through the particles without the need to pass through the matrix. To achieve this goal, it was sufficient to

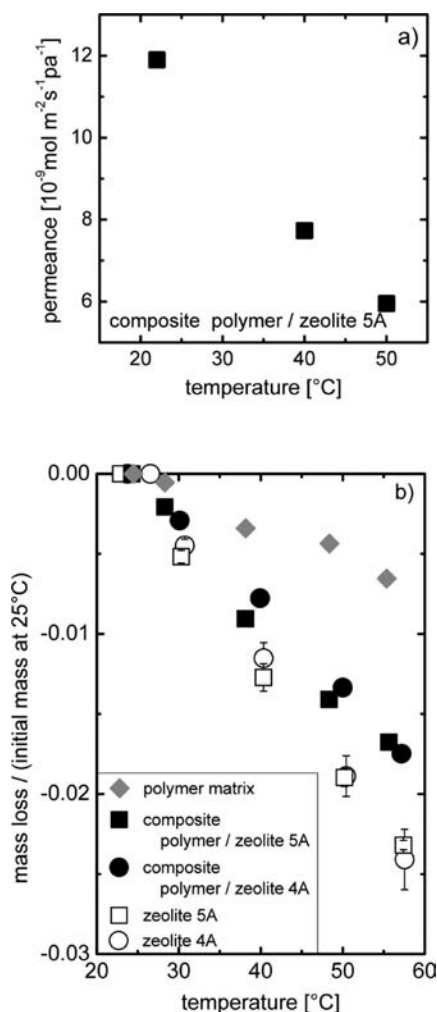


**Figure 9.** (a) Permeances of water at 23 °C, 40 °C, and 50 °C, through composite membranes made out of the polymeric matrix and zeolite 5A (■). (b) Relative weight loss occurring upon heating in presence of moist atmosphere of: pure zeolite 4A (○), pure zeolite 5A (□), bicontinuous composite membranes made out of the polymeric matrix and zeolite 4A (●), composite membranes made out of the polymeric matrix and zeolite 5A (■), and membranes made exclusively out of the polymeric matrix (grey ◆).

show selectivity for a pair of gases without caring about the commercial value of this particular selectivity. From here on, however, this technique opens a new possibility of embedding a variety of other highly selective but powdery materials into membranes in such a way that transport is possible predominantly through the selective material. Thus, in principle a wide variation of pore sizes and polarities might be implemented into flat polymeric membranes, including hydrophobic materials that are not filled with water, and finally lead to applications of technological importance and commercial value.

## AUTHOR INFORMATION

### Corresponding Author

werner.goedel@chemie.tu-chemnitz.de

### Notes

The authors declare no competing financial interest.

## ACKNOWLEDGMENTS

We thank A. Horvat (Silkem d.o.o., Kidričevo, Slovenia) for the contributed zeolite particles; Röhm Evonik GmbH for providing the monomer; A. Konrad (mecadi, Bexbach, Germany) and C. Staudt (University Düsseldorf, now BASF) for advice and support in setting up the permeation unit; and especially A. Konrad for providing a permeation cell. Furthermore, we thank M. Hietschold, S. Schulze, and G. Baumann from TU Chemnitz (Chair of Solid Surfaces Analysis) for help in obtaining the SEM images.

## REFERENCES

- (1) Caro, J.; Noack, M. Zeolite Membranes - Status and Prospective. *Advances in Nanoporous Materials*; Elsevier: Amsterdam, The Netherlands, 2010; Vol. 1, pp 1–96.
- (2) Snyder, M. A.; Tsapatsis, M. *Angew. Chem., Int. Ed.* **2007**, *46*, 7560–7573.
- (3) Xomeritakis, G.; Lai, Z.; Tsapatsis, M. *Ind. Eng. Chem. Res.* **2001**, *40*, 544–552.
- (4) Li, Y.; Chen, H.; Liu, J.; Li, H.; Yang, W. *Sep. Purif. Technol.* **2007**, *57*, 140–146.
- (5) Okamoto, K.; Kita, H.; Horii, K.; Tanaka, K.; Kondo, M. *Ind. Eng. Chem. Res.* **2001**, *40*, 163–175.
- (6) Berry, M. B.; Libby, B. E.; Rose, K.; Haas, K.-H.; Thompson, R. W. *Microporous Mesoporous Mat.* **2000**, *39*, 205–217.
- (7) Zimmerman, C. M.; Singh, A.; Koros, W. J. *J. Membr. Sci.* **1997**, *137*, 145–154.
- (8) Caro, J.; Albrecht, D.; Noack, M. *Sep. Purif. Technol.* **2009**, *66*, 143–147.
- (9) Yu, M.; Falconer, J. L.; Noble, R. D. *Ind. Eng. Chem. Res.* **2008**, *47*, 3943–3948.
- (10) Wang, H.; Huang, L.; Holmberg, B. A.; Yan, Y. *Chem. Commun.* **2002**, 1708–1709.
- (11) Jia, M.; Peinemann, K.-V.; Behling, R.-D. *J. Membr. Sci.* **1991**, *57*, 289–296.
- (12) Süer, M. G.; Bac und, N.; Yilmaz, L. *J. Membr. Sci.* **1994**, *91*, 77–86.
- (13) Boom, J. P.; Pünt, I. G. M.; Zwijnenberg, H.; de Boer, R.; Bargeman, D.; Smolders und, C. A.; Strathmann, H. *J. Membr. Sci.* **1998**, *138*, 237–258.
- (14) Cornelius, C.; Hibshman, C.; Marand, E. *Sep. Purif. Technol.* **2001**, *25*, 181–193.
- (15) Mahajan, R.; Koros, W. J. *Polym. Eng. Sci.* **2002**, *42*, 1432–144.
- (16) Hillock, A. M. W.; Miller, S. J.; Koros, W. J. *J. Membr. Sci.* **2008**, *314*, 193–199.
- (17) Moore, T. T.; Koros, W. J. *J. Mol. Struct.* **2005**, *739*, 87–98.
- (18) Lind, M. L.; Ghosh, A. K.; Jawor, A.; Huang, X.; Hou, W.; Yang, Y.; Hoek, E. M. V. *Langmuir* **2009**, *25*, 10139–10145.
- (19) Pendergast, M. T. M.; Ghosh, A. K.; Hoek, E. M. V. *Desalination* **2013**, *308*, 180–185.
- (20) This phenomenon is called particle-assisted wetting; without particles being present, the organic liquid monomer would form lenses instead of an even layer. Ding, A.; Goedel, W. A. *J. Am. Chem. Soc.* **2006**, *128*, 4930–4931.
- (21) Xu, H.; Goedel, W. A. *Langmuir* **2003**, *19*, 4950–4952.
- (22) Yan, F.; Goedel, W. A. *Chem. Mater.* **2004**, *16*, 1622–1626.
- (23) Xu, H.; Goedel, W. A. *Angew. Chem., Int. Ed.* **2003**, *42*, 4694–4696.
- (24) Values given are number averages obtained from at least 100 individual particles, and errors given are standard deviations.
- (25) The detection limit is given by the minimum pressure rise that can be detected, the waiting time between evacuations, the membrane thickness, and the feed pressure. For nitrogen and oxygen it is  $5 \times 10^{-12} \text{ mol m}^{-2} \text{ s}^{-1} \text{ Pa}^{-1}$ . The detection limit for water vapor is  $4 \times 10^{-11} \text{ mol m}^{-2} \text{ s}^{-1} \text{ Pa}^{-1}$ . Our detection limit for water is higher than the detection limit for nitrogen because the maximum water pressure to be used on the feed side is limited by the dewpoint. The pure



polymer membrane is thicker than the composite membrane; to reach the same detection limit, the waiting time was increased in an appropriate manner.

(26) Aoki, K.; Kusakabe, K.; Morooka, S. *Ind. Eng. Chem. Res.* **2000**, *39*, 2245–2251.

(27) Ruthen, D. M. *Microporous Mesoporous Mat.* **2012**, *162*, 69–79.

(28) Zhu, W.; Gora, L.; van den Berg, A. W. C.; Kapteijn, F.; Jansen, J. C.; Moulijn, J. A. *J. Membr. Sci.* **2005**, *253*, 57–66.

(29) In case of zeolites, there are reports that the unit cell contracts with decreasing water content: Sorenson, S. G.; Payzant, E. A.; Gibbons, W. T.; Soydas, B.; Kita, H.; Noble, R. D.; Falconer, J. L. *J. Membr. Sci.* **2011**, *366*, 413–420 This effect may as well give rise to a decrease in diffusion coefficient upon depletion of water.

(30) Sato, K.; Sugimoto, K.; Nakane, T. *J. Membr. Sci.* **2008**, *307*, 181–195.